Journal of Power Sources 221 (2013) 186–190

Contents lists available at SciVerse ScienceDirect

Journal of Power Sources

journal homepage: www.elsevier.com/locate/jpowsour

Short communication

Application of quinonic cathode compounds for quasi-solid lithium batteries

Yuki Hanyu, Yoshiyuki Ganbe, Itaru Honma*

Institute of Multidisciplinary Research for Advanced Materials, Tohoku University, Katahira 2-1-1, Aoba-ku, Sendai, Miyagi 980-8577, Japan

HIGHLIGHTS

- Three high energy-density quinonic cathode compounds were incorporated in solid-state organic cathode batteries.
- The cycleabilities of organic cathode cells were improved by nearly two orders of magnitude compared to conventional cells.
- The general applicability of organic cathode solid-state cells was demonstrated.
- Compounds that have been regarded "unusable" became "usable" under novel cell design and construction.

ARTICLE INFO

Article history:
Received 1 July 2012
Received in revised form
8 August 2012
Accepted 14 August 2012
Available online 21 August 2012

Keywords:
Organic cathode
Lithium battery
Solid-state battery
Ionic liquid
DDQ
Benzoquinone

ABSTRACT

Solid-state cells are one of the strongest candidate designs for utilisation of renewable high-capacity organic cathode materials. Following our previous work on tetracyanoquinodimethane, further high-capacity quinonic compounds, namely dichlorodicyanobenzoquinone, tetrahydroxybenzoquinone and dihydroxybenzoquinone were investigated. Cell cycling experiments indicated that these compounds undergo reversible redox reaction with significantly less cyclic capacity decay. 3.4 V of cell voltage was attainable from DDQ cells and capacities exceeding 250 mAh g^{-1} were obtained from THBQ and DHBQ. These results reassure that by adopting an appropriate battery design, cycleability of organic cathodes can be drastically improved and they can be exploited as low-cost environmentally friendly high energy-density cathode materials.

1. Introduction

Recent surge in demands for large-scale batteries in electric vehicles and "smart grid" applications require development of battery materials that are low-cost, free of resource restrictions and environmentally friendly. The Ni–Co–Mn oxide cathodes on the market today falls short for this purpose because they require "rare metals" such as Co and preparation involves energy-intensive processes [1]. On the contrary, organic compounds present promising possibilities because they are high energy density, free of metallic species, raw materials are renewable and processing is less energy intense [2,3]. However, practical application has been unsuccessful due to low cycleability, primarily owing to low conductivity, side reactions and dissolution into electrolyte. The side reaction and low conductivity can be mitigated by careful selection of compounds and appropriate use of conductive additives, but cathode dissolution remains as an obstacle. There have been attempts such as polymerisation [4–8], immobilisation by covalent bonding [9,10], physisorption [11,12], the use of radical polymers [13], to suppress the capacity loss, but important performance parameters such as energy density, rate performance or safety often had to be compromised one way or another. Adopting an all-solid design is one of the obvious strategies, but examples have been very limited to specific compounds [14].

We recently developed a general strategy to accommodate soluble quinonic cathode materials in quasi-solid cells, which electrolyte consisted of silica nanoparticles and room temperature ionic liquid (RTIL) [15]. It is anticipated that adoption of solid-state design provides more fundamental solution to the dissolution issue and enables the effective use of many monomeric compounds reported to date [3,16–18]. In addition to the previously reported tetracyanoquinodimethane (TCNQ), further candidate cathode compounds, namely 2,3,5,6-tetrahydroxybenzoquinone (THBQ), 2,3-dichloro-5,6-dicyano-benzoquinone (DDQ) and 2,5-dihydroxy benzoquinone (DHBQ) were integrated in test cells to characterise their battery performance. Quinones are well-known compounds

* Corresponding author. Tel.: +81 22 217 5816; fax: +81 22 217 5828.
E-mail address: i.honma@tagen.tohoku.ac.jp (I. Honma).

0378-7753/$ – see front matter © 2012 Elsevier B.V. All rights reserved.
http://dx.doi.org/10.1016/j.jpowsour.2012.08.040

and their cathode applications have been reported several times, but unmodified quinone tends to suffer low utilisation or rapid dissolution. DDQ has high electron affinity and redox potential due to aromaticity gain and charge delocalisation over electron-withdrawing substituents [19]. THBQ, which is a biomass-based material, has been studied in the past using conventional organic electrolyte such as propylene carbonate, vinylene carbonate etc [20]. The theoretical capacity of DHBQ is large, but due to its low molecular mass and high solubility, only its polymerised entity has been considered [21].

In this report, high energy-density solid-state cells of DDQ, THBQ and DHBQ were constructed to establish the methodology of using monomeric compounds for a cathode. Also, the rate and temperature dependence of cell performance was investigated to further pursue higher energy and power densities.

2. Experimental

2.1. Materials

DDQ, THBQ and DHBQ were purchased from TCI (Tokyo Kasei Corp.) and used without further purification. EC/DEC (1:1 mixture of ethylene carbonate and diethyl carbonate) 1 M $LiClO_4$ was purchased from Kishida Chemicals and stored under Ar atmosphere. 1-ethyl-3-methylimidazolium bis(trifluoromethanesulfonyl)amide ("[EMIm][Tf_2N]", Io-li-tec) was vacuum desiccated at 483 K for 3 h and stored under Ar until use.

2.2. Quasi-solid electrolyte

The detailed procedure for preparation of silica-RTIL composite quasi-solid electrolyte is described elsewhere [22]. The mean diameter of fumed silica nanoparticles was ~6 nm and silica-RTIL ratio was 1:3 by volume. The thickness and conductivity of solid electrolyte was typically around 400 μm and ~1×10^{-3} S cm^{-1} at room temperature (RT). Polyethylene oxide (PEO) membranes were prepared by dissolving PEG (MW = 6000), PEO (Mw = 4,000,000), and Li[Tf_2N] at 8:1:1 ratio in acetonitrile and vacuum drying at 343 K. The PEO residue was compressed at 2000 N at 333 K to form a film with a typical thickness of 20–30 μm. The cathode current collector was prepared by grinding a 4:1 mixture of acetylene black carbon (AB) and PTFE in pestle and mortar and drying under vacuum at 433 K.

2.3. Cathode preparation

The organic cathode pastes were prepared by blending quinonic compounds with Ketjen Black (KB, 1270 m^2 g^{-1}) and solution casting in THF. The quinone–KB mixture suspension in THF was dried at 363 K in air for 2 h and further by vacuum drying at 343 K. The residue was mixed with PTFE and manually ground using a pestle and mortar until paste formed. The typical thickness of such pastes was 200–300 μm.

2.4. Cell construction

The cathode-electrolyte combined disc was assembled by stacking solid electrolyte, PEO film, 3–4 mg of cathode paste (5–7 mm in diameter) and a carbon current collector disc in a die with the internal diameter of 10 mm. The entire stack was compressed in the die at ~100 MPa to form a pellet. 8 μl of [EMIm][Tf_2N] was dropped on the electrolyte side and the pellet was left in vacuum for ~15 min to remove any remaining bubbles. 5 μl of EC/DEC 1 M $LiClO_4$ was dropped on a freshly cut shiny lithium metal, left for ~15 min and the pellet was placed over. The cell was sealed in a CR2032 coin cell under argon atmosphere. Charge–discharge (C/D, also known as constant current cyclic voltammogram) measurements were conducted with Hokuto Denko HJ1001SD8 potentiostat.

2.5. Liquid cell construction

A U-shaped electrochemical cell was filled with EC/DEC with 1 M $LiClO_4$. A metallic lithium anode, reference electrode (3–4 cm^2) and cathode paste mounted on platinum mesh were immersed in the electrolyte. The C/D measurements were conducted using a Solartron 1400 Cell Test System.

3. Results and discussion

Cathode pastes containing ~75 wt.% of quinonic compounds, 20 wt.% conductive additive (Ketjen Black, "KB") and 5 wt.% binder (polytetrafluoroethylene, "PTFE") were prepared. Their theoretical capacities and estimated cell voltages are summarised in Table 1. Fig. 1 shows the SEM/EDX map of DDQ, THBQ and DHBQ cathode pastes. The typical dimension of DDQ and THBQ crystals were 3–5 μm and that of DHBQ were ~20 μm (Supplementary Fig. S1). The spatial distribution of DDQ, THBQ and DHBQ was determined by chlorine or oxygen signal distribution (Fig. 2). The DDQ showed highly homogeneous distribution of Cl signals. The THBQ showed generally homogeneous distribution, but crystal grains showing as "hotspots" of oxygen signals were also observed. DHBQ was also generally homogeneous and oxygen signal hotspots were rare. Upon SEM/EDX imaging, local charge accumulation did not occur even without gold deposition. This indicated that conductive additives provided sufficient electronic conductivity to cathode. This is a desirable or necessary property for a battery using insulating active materials.

3.1. Cell assembly and battery performance

Cells were assembled by stacking silica-composite quasi-solid electrolyte, PEO layer, cathode paste and carbon paste current collector and compressing together into a pellet at 100 MPa [15]. After wetting the pellet with RTIL, metallic lithium anode was mounted and a cell was assembled [15]. In the first sequence of cell characterisation, active compound fractions were set to ~50% and C/D measurements (constant current cyclic voltammogram) were carried out at RT and 0.2 C rate. Measurements were conducted both in liquid electrolyte cells and solid-state cells. The potential profiles and cycleability properties were then compared and analysed to verify reversible battery reactions (Fig. 3).

A cell using a DDQ paste (67.1 wt.% DDQ, 26.9 wt.% KB, 6.0 wt.% PTFE) was constructed and evaluated in a liquid cell. Two potential plateaus near 3.4 V and 3.2 V, which corresponded to the first and second redox potentials, appeared. However, the specific capacity was only 50 mAh $g^{-1}{}_{-DDQ}$ for the first cycle and the subsequent

Table 1
Theoretical capacity and cell voltages of DDQ, THBQ and DHBQ measured by liquid cell experiments. Theoretical energy densities were calculated accordingly.

	DDQ	THBQ	DHBQ
Molecular structure	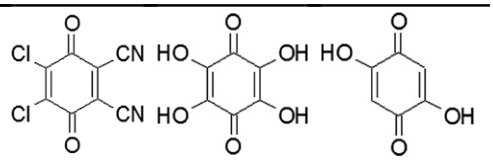		
Theoretical capacity	237 mAh g^{-1}	311 mAh g^{-1}	382 mAh g^{-1}
Cell voltage	3.6–3.0 V	3.0–1.6 V	3.2–1.8 V
Energy density	~750 Wh kg^{-1}	~800 Wh kg^{-1}	~950 Wh kg^{-1}

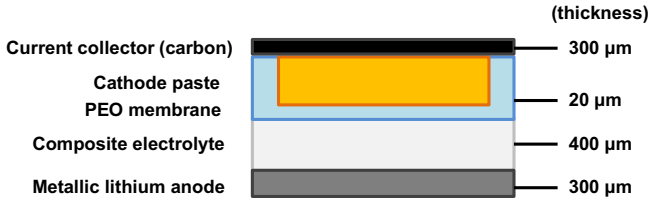

Fig. 1. The schematic of a solid-state cell hosting organic cathode. The PEO membrane and composite electrolyte prevents cathode dissolution and carbon current collector encapsulates the cathode body.

cyclic decay was rapid (Supplementary Fig. S2A). The cathode dissolution was also evident from the change in colour of initially colourless EC/DEC electrolyte into the yellow colour of DDQ. Hence, DDQ was practically unusable in organic liquid electrolyte.

On the contrary, a solid cell under the same conditions (0.2 C, RT) demonstrated the reversible battery reaction of DDQ by showing nearly 100% coulombic efficiency at ~160 mAh g^{-1}_{-DDQ} specific capacity (Fig. 2). The cathode contained ~2 mg of DDQ and the estimated current density was ~0.3 mA cm^{-2}. The first 3.4 V plateau was visible in the discharge profile, but the second 3.2 V plateau was obscure. The capacity slightly increased from the 1st to 2nd cycle, probably due to permeation of RTIL in cathode body and interfacial layer formation. It is also known that the first C/D cycle tends to exhibit low coulombic efficiency due to decomposition of electrolyte form solid–electrolyte interface on the anode. The capacity was short of the theoretical value, 236.5 mAh g^{-1}_{-DDQ}. Since the separation between charge and discharge plateaus (polarisation) were not excessively large, it was unlikely that solid electrolyte thickness was the primary obstacle for battery reaction. Rather, it appeared that the second redox reaction ($Li + [Li^+][DDQ^-] \rightarrow [Li^+]_2[DDQ^{2-}]$) was the bigger obstacle. A possible reason is because Li-DDQ crystals are highly insulating to electrons and Li-ions and does not yield to fast second redox reaction. If such is the case, an improved cathode preparation method may grant better electron or Li-ion access. This might attain higher cathode utilisation ratio, possibly at a higher fraction of DDQ.

A THBQ paste (47.6 wt.% THBQ, 48.3 wt.% KB, 4.1 wt.% PTFE) was evaluated likewise. In a liquid cell, a clear-cut potential plateau corresponding to the first redox potential that lay near 2.8 V. The peak for second redox potential was smaller and less obvious but was clearly present near 2.4 V. The highest specific capacity was ~170 mAh g^{-1} (Supplementary Fig. S2B).

For a solid cell, the highest attainable capacity was ~290 mAh g^{-1} and for the next ten cycles, ~250 mAh g^{-1} of capacity was maintained. By raising the temperature to 323 K, the theoretical capacity (311.5 mAh g^{-1}_{-THBQ}) was achieved at similar cycleability (Supplementary Fig. S3). These results are indicative of completely reversible cathodic reaction of THBQ. Under both temperatures, the initial cell voltages were near 2.8 V, but potential plateaus expected at 2.8 V and 2.4 V were not very evident. Instead, a gradually decreasing discharge profiles were observed. We relate this phenomenon to battery reactions occurring in solid phase as well as the contributions of restricted Li^+ transport in a quasi-solid cell [15].

The molecular mass of DHBQ (140.7 g mol^{-1}) is smaller than that of THBQ and the first redox potential is slightly higher (2.9 V for DHBQ, 2.8 V of THBQ). Accordingly, DHBQ possesses higher specific capacity and gravimetric energy density (382.6 mAh g^{-1}_{-DHBQ} and ~950 Wh kg^{-1}). In a liquid cell, the first redox potential was in fact, higher than that of THBQ, but the same dissolution problem as DDQ and THBQ hampered its use in batteries (Supplementary Fig. S2C). As before, solid-state design improved the battery performance. The specific capacity of a solid cell hosting DHBQ cathode (44.6 wt.% DHBQ, 48.3 wt.% KB, 7.3 wt.% PTFE) exhibited ~300 mAh g^{-1} initial capacity and higher average voltage with relatively small polarisation (Fig. 2C). Overall, DHBQ solid cell had 20–30% higher energy density than that THBQ cell. Nonetheless, the gradual change in discharge profiles over cycles and drop of average voltage still required investigation.

3.2. Power density and rate properties

A high weight fraction of cathode compound in a cathode body yields high energy density, but power density is often sacrificed due

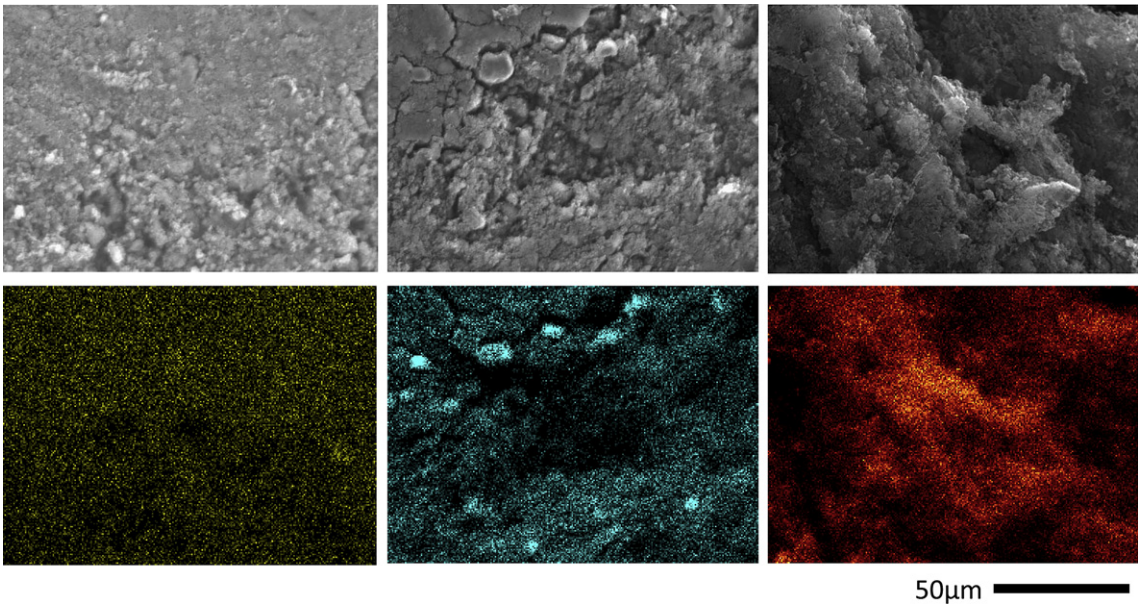

Fig. 2. SEM and EDX images of DDQ (left), THBQ (centre) and DHBQ (right) cathode paste at ×1000 magnification – the elements mapped are Cl for DDQ, O for THBQ and O for DHBQ. The distribution of Cl is highly uniform. The distribution of O in THBQ is mostly homogeneous, with some local concentrations. The distribution of DHBQ is heterogeneous over tens of μm.

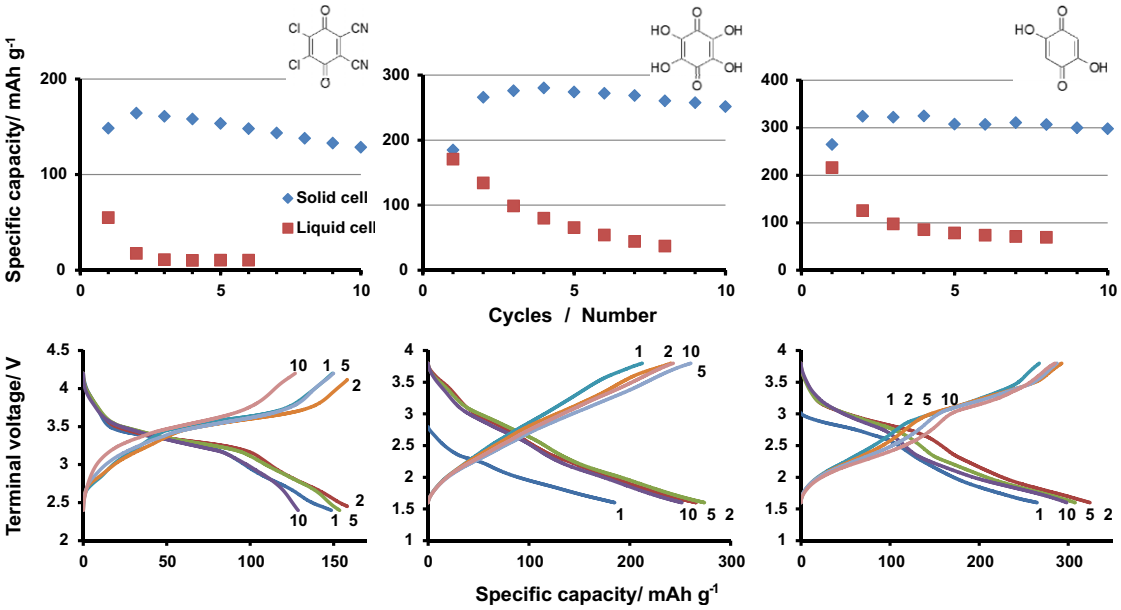

Fig. 3. Comparison of discharge capacities between liquid and solid cells of DDQ (left), THBQ (centre) and DHBQ (right) and C/D profiles of solid cells. The 1st, 2nd, 5th and 10th cycles are presented here. All compounds displayed reversible cathodic reactions in solid cells. THBQ and DHBQ cells reached 70–80% of the theoretical capacity at RT, but DDQ appeared to have undergone only the first redox reaction. The cathode compositions were DDQ:KB:PTFE = 67.1:26.9:6.0, THBQ:KB:PTFE = 47.6:48.3:4.1 and DHBQ:KB:PTFE = 44.6:48.3:7.3.

to compromised electronic contacts within cathode. This intricate balance between energy and power density has been a common reason for organic cathodes to contain low fraction of active compound [23]. While such measure also mitigates capacity loss by delaying dissolution, it reduces the energy density of a cathode body as a whole. Regarding active material content, a quasi-solid cell demonstratively accommodated 45 wt.% or higher while preventing dissolution and capacity loss. To investigate the possibility of even higher energy density, the fraction of active compounds were further raised to ~70 wt.%. The power densities were evaluated by cycling test cells at 0.2 C, 0.5 C, 1 C and 2 C at RT and 323 K and their specific power densities were estimated (Fig. 4).

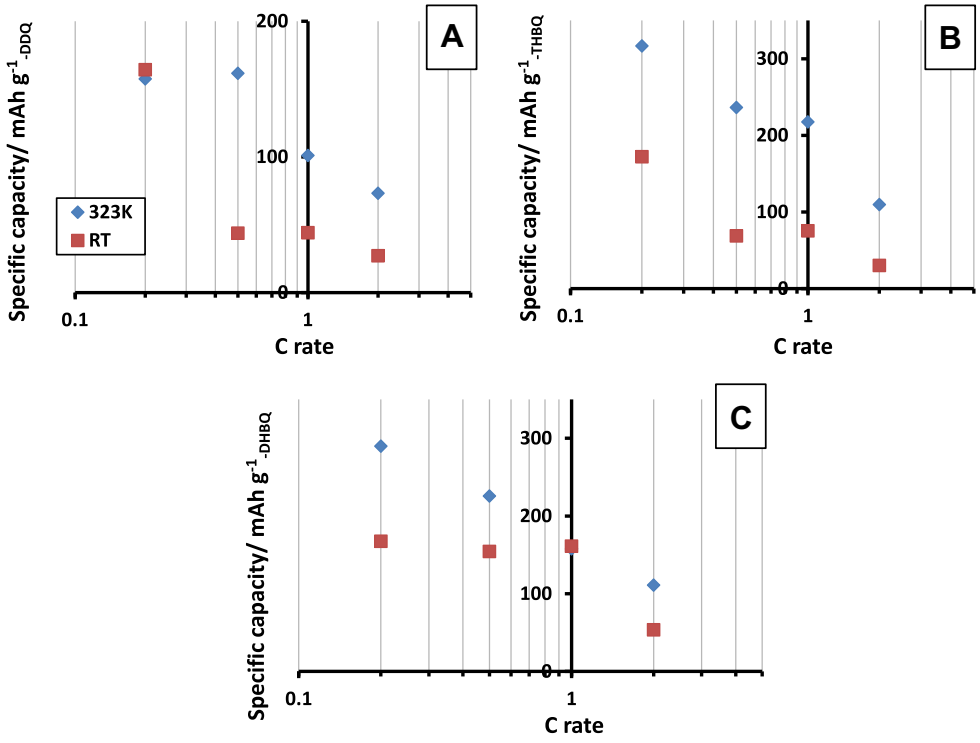

Fig. 4. The rate performance and power densities of solid-state organic cathode cells using DDQ (A), THBQ (B) and DHBQ (C) – datapoints represent the capacity of second discharge capacities at two temperatures. The fraction of active materials were 67.1 wt.%, 66.6 wt.% and 68.6 wt.% respectively. The highest power density of 540 Wh kg^{-1} occurred in THBQ cell at 323 K, at 1 C rate (~1.5 mA cm^{-2}).

The initial specific capacities were generally higher at increased temperatures, probably due to facilitated mass transport and faster redox reactions. Despite the increase of active compound fraction from ~45 wt.% to ~70 wt.%, THBQ and DHBQ at 0.2 C, 323 K recorded comparable specific capacities. Essentially, conductive additives reduced to ~25 wt.% provided sufficient electronic contact for organic crystals to undergo battery reactions. When C/D rate was increased from 0.2 C to 0.5 C, the DDQ cell maintained its capacity while THBQ and DHBQ showed lower capacities. This was probably because the first redox reaction of DDQ (that consisted most part of the near 160 mAh $g^{-1}{}_{-DDQ}$ capacity) was relatively fast and tolerated larger current density. But overall, the highest power density achieved in this set of experiment was 540 Wh kg^{-1} from a THBQ cell at 1 C rate.

4. Conclusion

3 Quinonic compounds, DDQ, THBQ and DHBQ, were integrated in quasi-solid state organic cathode lithium cells. By preventing cathode dissolution, these compounds exhibited improvements in cycleability by about two orders of magnitude. Moreover, experiments with DDQ demonstrated that compounds that may appear "unusable" in organic liquid electrolytes may become "usable" under the solid-state design. Yet, the cathodic reaction of DDQ was limited to the first redox reaction in a solid cell. THBQ and DHBQ showed high utilisation ratio even in cathodes containing ~70 wt.% of these species. Since solid electrolyte has not appeared to limit the cell performance, it is envisaged that improving cathode conductivity may achieve better rate performance or further increase in active material content.

Acknowledgements

This work was conducted under the financial support of the Funding Program for World-Leading Innovative R&D on Science and Technology (FIRST), under the Cabinet Office, Government of Japan.

Appendix A. Supplementary data

Supplementary data associated with this article can be found, in the online version, at http://dx.doi.org/10.1016/j.jpowsour.2012.08.040.

References

[1] P. Poizot, F. Dolhem, Energy Environ. Sci. 4 (2011) 2003–2019.
[2] M. Armand, J. Tarascon, Nature 451 (2008) 652–657.
[3] Y. Liang, Z. Tao, J. Chen, Adv. Energy Mater. 2 (2012) 742–769.
[4] J. Zhang, Z. Song, L. Zhan, J. Tang, H. Zhan, Y. Zhou, C. Zhan, J. Power Sources 186 (2009) 496–499.
[5] L. Zhan, Z. Song, J. Zhang, J. Tang, H. Zhan, Y. Zhou, C. Zhan, Electrochim. Acta 53 (2008) 8319–8323.
[6] X. Yu, J. Xie, J. Yang, H. Huang, K. Wang, Z. Wen, J. Electroanal. Chem. 573 (2004) 121–128.
[7] Z. Song, H. Zhan, Y. Zhou, Chem. Commun. (2009) 448–450.
[8] T. Le Gall, K.H. Reiman, M.C. Grossel, J.R. Owen, J. Power Sources 119-121 (2003) 316–320.
[9] K. Pirnat, R. Dominko, R. Cerc-Korosec, G. Mali, B. Genorio, M. Gaberscek, J. Power Sources 199 (2012) 308–314.
[10] B. Genorio, K. Pirnat, R. Cerc-Korosec, R. Dominko, M. Gaberscek, Angew. Chem. Int. Ed. 49 (2010) 7222–7224.
[11] Z. Lei, W. Wei-kun, W. An-bang, Y. Zhong-bao, C. Shi, Y. Yu-sheng, J. Electrochem. Soc. 158 (2011) A991–A996.
[12] T. Matsunaga, T. Kubota, T. Sugimoto, M. Satoh, Chem. Lett. 40 (2011) 750–752.
[13] T. Suga, H. Ohshiro, S. Sugita, K. Oyaizu, H. Nishide, Adv. Mater. 21 (2009) 1627–1630.
[14] S. Renault, J. Geng, F. Dolhem, P. Poizot, Chem. Commun. 47 (2011) 2414–2416.
[15] Y. Hanyu, I. Honma, Sci. Rep. 2 (2012).
[16] M. Yao, M. Araki, H. Senoh, S. Yamazaki, T. Sakai, K. Yasuda, Chem. Lett. 39 (2010) 950–952.
[17] M. Yao, H. Senoh, M. Araki, T. Sakai, K. Yasuda, ECS Trans. 28 (2010) 3–10.
[18] J. Geng, J. Bonnet, S. Renault, F. Dolhem, P. Poizot, Energy Environ. Sci. 3 (2010) 1929–1933.
[19] E.C.M. Chen, W.E. Wentworth, J. Chem. Phys. 63 (1975) 3183–3191.
[20] H. Chen, M. Armand, G. Demailly, F. Dolhem, P. Poizot, J. Tarascon, ChemSusChem 1 (2008) 348–355.
[21] J. Xiang, C. Chang, M. Li, S. Wu, L. Yuan, J. Sun, Crystal Growth Des. 8 (2007) 280–282.
[22] A. Unemoto, Y. Iwai, S. Mitani, S. Baek, S. Ito, T. Tomai, J. Kawamura, I. Honma, Solid State Ionics 201 (2011) 11–20.
[23] Y. Morita, S. Nishida, T. Murata, M. Moriguchi, A. Ueda, M. Satoh, K. Arifuku, K. Sato, T. Takui, Nat. Mater. 10 (2011) 947–951.